Structural and Biochemical Consequences of NF1 Associated Non-Truncating Mutations in the Sec14-PH Module of Neurofibromin

Stefan Welti, Sonja Kuehn, Igor d'Angelo, Britta Bruegger, Dieter Kaufmann, Klaus Scheffzek

Human Mutation

Structural and Biochemical Consequences of NF1 Associated Non-Truncating Mutations in the Sec14-PH Module of Neurofibromin

Journal:	*Human Mutation*
Manuscript ID:	humu-2010-0383.R1
Wiley - Manuscript type:	Research Article
Date Submitted by the Author:	19-Oct-2010
Complete List of Authors:	Welti, Stefan; European Molecular Biology Laboratory, Structural and Computational Biology Unit Kuehn, Sonja; European Molecular Biology Laboratory, Structural and Computational Biology Unit D'Angelo, Igor; European Molecular Biology Laboratory, Structural and Computational Biology Unit Bruegger, Britta; Biochemistry Center Heidelberg (BZH), Vesicular Transport Kaufmann, Dieter; University, Institute of Human Genetics Scheffzek, Klaus; European Molecular Biology Laboratory (EMBL), Structural and Computational Biology Unit
Key Words:	neurofibromatosis type 1, pleckstrin homology , Sec14, tumor suppressor, X-ray crystallography, mass spectrometry, glycerophospholipid, missense mutation, non-truncating mutation

Structural and Biochemical Consequences of NF1 Associated Non-Truncating Mutations in the Sec14-PH Module of Neurofibromin

Stefan Welti[1]*, Sonja Kühn[1,4], Igor D'Angelo[1,4], Britta Brügger[2], Dieter Kaufmann[3], Klaus Scheffzek[1]*

[1]European Molecular Biology Laboratory (EMBL), Structural and Computational Biology Unit, Meyerhofstrasse 1, 69117 Heidelberg, Germany

[2]Biochemistry Center Heidelberg (BZH), Im Neuenheimer Feld 328, 69120 Heidelberg, Germany

[3]Institute of Human Genetics, University of Ulm, Albert-Einstein-Allee 11, 89070 Ulm, Germany

[4]Present addresses: (I.D'A.)Zymeworks Inc., 540-1385 West 8th Avenue, Vancouver BC V6H 3V9, Canada; (S.K.) Max-Planck-Institute f. Molecular Physiology, Otto-Hahn-Str. 11, 44227 Dortmund, Germany

Corresponding authors:

* scheffzek@embl.de or welti@embl.de

Key Words: neurofibromatosis type 1, Sec14, pleckstrin homology, glycerophospholipid, X-ray crystallography, missense mutation, mass spectrometry, tumor suppressor

Abstract

Neurofibromatosis type 1 (NF1) is a common genetic disorder caused by alterations in the tumor suppressor gene *NF1*. Clinical manifestations include various neural crest derived tumors, pigmentation anomalies, bone deformations and learning disabilities. *NF1* encodes the Ras specific GTPase activating protein (RasGAP) neurofibromin, of which the central RasGAP related domain as well as a Sec14-like (residues 1560-1699) and a tightly interacting pleckstrin homology (PH)–like (1713-1818) domain are currently well defined. However, patient-derived ~~missense~~ non-truncating mutations have been reported along the whole *NF1* gene, suggesting further essential protein functions. Focusing on the Sec14-PH module, we have engineered such non-truncating mutations and analyzed their implications on protein function and structure using lipid binding assays, CD spectroscopy and X-ray crystallography. While lipid binding appears to be preserved among most non-truncating mutants, we see major structural changes for two of the alterations. Judging from these changes and our biochemical data, we suggest the presence of an additional intermolecular contact surface in the lid-lock region of the protein.

Introduction

The common genetic disorder neurofibromatosis type1 (NF1, MIM: #162200) is a familial cancer syndrome that is characterized by a high incidence of neurofibromas, bone deformations, pigmentation anomalies, learning disabilities and a number of additional features (Riccardi, 1992; Upadhyaya and Cooper, 1998) that contribute to a rather complex disease phenotype. Alterations in the tumor suppressor gene *NF1* (HGNC:7765, MIM: *613113, RefSeq: NM_000267.3), encoding the cytoplasmic protein neurofibromin (320 kDa, 2818aa, RefSeq: NP_000258.1, UniProtKB P21359-2)(Le and Parada, 2007; McClatchey and Cichowski, 2001; Viskochil, et al., 1993; Zhu and Parada, 2001), are responsible for the pathogenesis of NF1. Neurofibromin is a Ras specific GTPase activating protein (RasGAP) with a central segment termed GAP related domain (GRD, Figure 1a) that has been extensively characterized in numerous laboratories including ours (Cichowski and Jacks, 2001; Scheffzek, et al., 1998; Zhu and Parada, 2001). Of the mutational spectrum of NF1 the majority of alterations found in NF1-patients result in premature stop codons most likely leading to elimination of the transcript by the RNA surveillance machinery or to truncated peptides incompatible with a functional protein. Approximately 10% of alterations are compatible with a missense mutated protein, although the production of such protein has not been verified in many cases (Fahsold, et al., 2000; Shen, et al., 1996). Largely, the missense mutations are distributed uniformly over neurofibromin, with clusters in the GRD region and the so-called cysteine-serine-rich-domain (CSRD, Figure 1a) (Izawa, et al., 1996), suggesting this domain to be of functional importance as well (Fahsold, et al., 2000). While numerous binding partners of neurofibromin have been reported (Patrakitkomjorn, et al., 2008; Phan, et al., 2010; Welti, et al., 2008), the physiological significance of the underlying protein-protein

interactions remains largely unclear. Using structural biology approaches we have previously discovered a bipartite module at the C-terminus of the GRD (D'Angelo, et al., 2006, Figure 1a). It is composed of an N-terminal, lipid binding Sec14- and a C-terminal PH-like portion that appear to form a regulatory interface, presumably to modulate ligand binding of the Sec14-like domain (D'Angelo, et al., 2006; Welti, et al., 2007). A number of missense mutations of the Sec14-PH module have been identified in NF1-patients as well as single and double amino acid deletions (Table 1). In addition a tandem duplication (TD, see Table 1) of 14 amino acids was observed with the affected patients displaying features linked to Watson- and Noonan syndrome (Tassabehji, et al., 1993). Mapping these alterations onto the Sec14-PH structure suggests moderate structural changes in most cases. In contrast, deletion or insertion mutants as found in exposed regions are unlikely to leave the structure unchanged. In order to define/model the local effect of NF1 associated non-truncating mutations and to investigate whether they would interfere with lipid binding or protein stability we have overexpressed and purified the respective Sec14-PH-mutants from an *E. coli* expression system. Purified proteins were subject to biochemical analysis including CD spectroscopy and lipid binding assays monitored by mass spectrometry. Selected mutants of potential structural impact were analyzed by X-ray crystallography, for two of which we also demonstrate normal mRNA and protein levels in patient-derived cultured cells.

Materials and Methods

Nucleotide and codon numbering is based on the cDNA reference sequence. Codon 1 is the initiation codon ATG with the Nucleotides +1 to +3, according to journal guidelines (www.hgvs.org/mutnome).

Cloning, Expression and purification of HsNF1 Sec14-PH and variants: The Sec14-PH region (residues 1545-1816) of human neurofibromin (Bonneau, et al., 2004; D'Angelo, et al., 2006; Welti, et al., 2007) was amplified from cDNA by PCR and cloned (Sambrook and Russell, 2001) into the pETM11 expression vector (EMBL, protein expression and purification core facility). All deletion and point mutations were made by using the Quickchange site-directed mutagenesis kit (Stratagene) following manufacturer's instructions. The tandem duplication mutant TD was generated via two PCR reactions (see primers, Supp. Table S1) amplifying the 3' and 5'-half of the coding sequence with the central primers containing addition nucleotides for the duplication and a terminal BsaI restriction site. The PCR products were digested with NcoI+BsaI or NotI+BsaI, purified and ligated into a pETM11 vector predigested with NcoI/NotI. For expression, the wild-type protein and variants were grown in BL21 CodonPlus(DE)-RIL *E. coli* cells (Stratagene) to an OD_{600} of 0.8-1.0, induced with 0.2 mM IPTG and incubated over night (18 h, 291K, 200 rpm). Cell lysis was done by 10 min incubation in buffer LyB (20 mM Tris, 0.5 M NaCl, 40 mM Imidazol, pH8.1) with 1 µg/ml Lysozym (Sigma-Aldrich) and DNaseI (Roche), followed by sonication (5x2 min, duty cycle 50%, power 5; Branson W-250, Heinemann). After an ultracentrifugation step (40.000 rpm, 1 h , 277K), the cell lysate was continuously applied to a pre-equilibrated 1 ml HisTrap column (GE healthcare) in a circulatory way for 2 h and washed with 10 ml buffer LyB. Following

elution with 10 ml buffer EB (20 mM Tris, 0.5 M NaCl, 125 mM imidazol, pH8.1), the protein solution was incubated with TEV-Protease (28 h, 5 µg/mg protein, 277K) for cleavage of the His-tag, concentrated to a volume of 2 ml (AmiconUltra-15, 10K MWCO, Milipore) and subjected to preparative size exclusion chromatography (GE healthcare, Superdex 200 HiLoad 16/60) with buffer GF (20 mM Tris, 150 mM NaCl, 1 mM EDTA, pH8.0). Afterwards, protein containing fractions were concentrated to 10 mg/ml (as above) and stored at 193K after flash freezing in liquid nitrogen.

Analytical size exclusion chromatography: Ca 250 µg protein in buffer GF was applied to a size exclusion chromatography column (GE healthcare, Superdex 200, 25 ml column volume) calibrated with BioRad gelfiltration standard. The resulting curves were normalized and analyzed with Excel (Microsoft).

Circular dichroism spectroscopy: From 40-120 µg of protein in PBS buffer (pH 7.4) CD-spectra were recorded in a range from 199-250 nm (Jasco-710 spectropolarimeter; Helmann 100-QS/110-QS quarz precision cuvette) with 1 nm resolution, 20 mdeg sensitivity and 10 accumulations at 293K. To measure the thermal stability of proteins, the CD-signal at 205 nm was recorded during an increase of temperature from 293 to 353K at a rate of 1K/min. The recorded data was processed and analyzed with Excel (Microsoft).

Protein-lipid overlay assays: As described before (D'Angelo, et al., 2006), PIP-Strips or Sphingo-Strips (Echelon Biosciences Inc., Salt Lake City, UT, USA) were blocked o/n in buffer PipB (PBS pH6.0, 0.1% Tween-20 (Sigma-Aldrich)) plus 3% fatty acid free BSA (Sigma-Aldrich), incubated 1 h after addition of 10 µg Protein and

washed 10x 5 min with buffer PipB. Detection was done with Rabbit anti-NF1 Sec14-PH antibody (1:1000, 1 h, buffer PipB + BSA), washing (2x 1 min, 1x 1 h, 3x 10 min buffer PipB), HRP-coupled anti-rabbit antibodies (Sigma-Aldrich, 1:10'000, 1 h, buffer PipB + BSA), washing (3x 1 min, 1x 1 h, 4x 5 min, buffer PipB) and the ECLplus kit (Amersham) following manufacturer's instructions. Overlay assays were done at 277K.

Liposome preparation, lipid exchange assay and mass spectrometry: The preparation of liposomes, lipid exchange assays and extraction of lipids from protein samples for MS analysis was done as previously described (Welti, et al., 2007). Liposomes consisted of 6.88% Sphingomyelin (SM, brain); 14.27% 1,2-dioleoyl-*sn*-glycero-3-phosphocholine (DOPC); 54.28% 1-palmitoyl(D31)-2-oleoyl-*sn*-glycero-3-phosphoethanolamine (D31PE); 22.17% L-α-phosphatidylinositol (PI, bovine liver) and 2.45% 1,2-dioleoyl-*sn*-glycero-3-phospho-L-serine (DOPS, all lipids from Avanti Polar lipids inc.) mimicking thereby the lipid composition of the inner leaflet of plasma membranes as observed in mammalian cells (Calderon and DeVries, 1997).

For lipid mass spectrometry, samples were extracted in the presence of internal standards (Brugger, et al., 2006). After solvent evaporation, the samples were resuspended in 10 mM ammonium acetate in methanol. Quantification of lipids was performed in positive ion mode on a triple-stage quadrupole tandem mass spectrometer (QII, Micromass) equipped with a nano-ESI source (Z spray). Argon was used as collision gas at a nominal pressure of 2.5 x 10^{-3} millibar. The cone voltage was set to 30 V (50 V for PC analysis). The quadrupoles Q1 and Q3 were operated at unit resolution. Detection of PC was achieved by precursor ion scanning for the fragment ion m/z 184 at a collision energy (CE) of 32 eV. PE, PI, PS, and PG

measurements were carried out by scanning for neutral losses of m/z 141 (CE: 20 eV), m/z 277 (CE: 30 eV), m/z 185 (CE: 20 eV), and m/z 189 (CE: 20 eV), respectively.

Crystallization and structure determination: Crystals were grown at room temperature (~291K) using the hanging-drop method commonly mixing equal volumes of protein (1 µl, ~7-15 mg/ml) and reservoir solution of the following compositions for the respective mutants: ***p.I1584V***: 0.1 M MES pH6.0, 7.5% PEG 4000, 0.2 M $Na_4P_2O_7$; ***TD***: 0.05 M HEPES pH7.0, 39% PEG 400 (Fluka), 0.2M $(NH_4)_2SO_4$; ***p.K1750del***: 0.1 M MES pH6.0, 0.25 M $Na_4P_2O_7$, 13% PEG 4000. Datasets were collected under cryogenic conditions (100 K) at the European Synchrotron Radiation Facility Grenoble (ESRF) and processed with XDS (Kabsch, 1993). For structure determination, the wild-type HsNF1 Sec14-PH structure (Welti, 2007; PDB code 2E2X) was used either directly as starting model for refinement or as search model in molecular replacement calculations using CNS (Brunger, et al., 1998) in case of TD1699-1713. Refinement was carried out with CNS, CCP4/Refmac (CCP4, 1994; Murshudov, et al., 1997) or Phenix (Adams, et al., 2002), alternating with manual rebuilding using COOT (Emsley and Cowtan, 2004). TLS groups were selected based on analysis with TLSMD (Painter and Merritt, 2006; Painter, 2006). A summary of the crystallographic analysis is presented in Table 2.

Quantification of neurofibromin from patient-derived cultured cells:

The investigated NF1-patients correspond to the NIH criteria and gave informed consent prior to the blood isolation. The 28 and 35-year old sporadic NF1 patients exhibited typical symptoms of NF1: more than 100 cutaneous and subcutaneous

neurofibromas, multiple café au lait macules, axillary freckles and Lisch nodules bilaterally. Both are not affected by severe complications of the disease. Neurofibromin amounts were assessed by immunoprecipitation using equal amounts of total protein (250 or 500 µg) from cultured peripheral blood cells of NF1-patients and controls. Detection of the protein was done by Western-blot analysis (Griesser, et al., 1997) using the sc-67 and sc-68 antibodies from Santa Cruz Biotechnology. As described previously (Kaufmann, et al., 1999a), the expression levels of p120-GAP and ß-tubulin were analyzed as control. Resulting protein bands were quantitatively evaluated by video-densitometry.

Results and Discussion

NF1 associated ~~missense~~ non-truncating mutations of the Sec14-PH module were engineered by site directed mutagenesis of the human Sec14-PH coding sequence, expressed in *E. coli* and purified as described in the Methods section. Apart from a few exceptions (see below), the majority of the mutants was soluble and folded as confirmed by size exclusion chromatography and CD spectroscopy, allowing the assessment of lipid binding and exchange activity. Expression of mutants was analyzed in human cultured peripheral blood cells if source material was available. Three prominent mutations based on their location in the structure and/or due to availability of clinical data were analyzed by X-ray crystallography.

Most NF1-associated Sec14-PH non-truncating mutations retain exchange of glycerophospholipids

The engineered non-truncating mutations were subject to lipid exchange assays

using liposomes mimicking the lipid composition of the plasma membrane inner leaflet of Schwann Cells. After exchange, the protein lipid content was analyzed by nano-ESI mass spectrometry. The results indicate no major change in the composition of bound lipids compared to that of the wild-type Sec14-PH module (Supp. Figure S1). Interestingly most mutations located close to the Sec14 lipid binding pocket were poorly soluble in our production scheme, suggesting that interfering with the structure of the lipid binding pocket may disrupt essential structural elements.

NF1-p.K1750del and p.I1584V mutant proteins are fully expressed in patients

We investigated the stability of mutated neurofibromin in cells of NF1-patients with the suggested ~~missense~~ non-truncating mutations NF1-p.K1750del (exon 29, c.5248_5250delAAA) and NF1-p.I1584V (exon 27b, c.4750A>G)(Fahsold, et al., 2000). Using immunoprecipitation and Western Blot experiments, we showed that the total amount of expressed neurofibromin is not reduced in two NF1-patients compared to healthy donors (Figure 2). These data were confirmed by real-time RT-PCR investigations of *NF1* mRNA levels in cells of these patients, indicating unchanged expression levels (data not shown). Since the amounts of mRNA and protein are not reduced or increased compared to the wild-type situation, we conclude that the two alterations represent functional non-truncating mutations. Their pathogenic effect might be caused rather by modification or disruption of intra- or intermolecular protein-protein / ligand interaction surfaces than by mRNA degradation, decrease of protein stability or insolubility.

Recombinant Sec14-PH(p.K1750del) and (p.I1584V) modules are folded

comparable to the wild-type protein

To investigate potential biochemical consequences of the patient-derived mutations of neurofibromin, we expressed and purified appropriate protein constructs of the Sec14-PH region (Supp. Figure S2). To verify the integrity of the purified mutants, we subsequently assessed their oligomeric state by analytical gelfiltration (Supp. Figure S3), the overall fold with CD spectroscopy (Supp. Figure S4) and their stability by thermal denaturation experiments (Supp. Figure S5). The analyzed properties of mutants were not impaired, with the exception of the thermal stability of TD and p.K1750del, which was significantly lowered (Table 1). While the wild-type protein unfolds at about 335K in our experimental setup, both mutants become unstable already at 325K, suggesting a higher flexibility of local segments of the proteins. Overall, the analyzed constructs are comparable to the wild-type module, further supporting the hypothesis that the associated pathogenic effects are likely to be mediated by local disruptions of neurofibromin functions. The obtained results are as well compatible with our observations that neither p.K1750del and p.I1584V lead to cellular neurofibromin degradation on the pre- or posttranslational level in cells derived from patient material ~~with the clinical data available for p.K1750del and p.I1584V~~, thus complementing these findings biochemically.

Structural consequences of selected engineered patient-derived mutations (p.K1750del, TD, p.I1584V)

Mutant proteins were purified, crystallized and their structures solved as described in the methods section. The crystallographic analysis is summarized in Table 2. The overall structure is largely similar to that of the wild type Sec14-PH portions (D'Angelo, et al., 2006; Welti, et al., 2007, Figure 1b) with local alterations due to the

introduced changes as described below.

p.K1750del: The deletion p.K1750del is significantly rearranging a loop of the PH-like domain, previously termed β-protrusion ('lock') and most likely controlling the flexibility of the helical segment ('lid') that covers the presumed entry site for the lipid binder (D'Angelo, et al., 2006). Structurally, the deletion is associated with a peptide flip (Figure 1d) that place the preceding residue in the position of the former K1750 and moves R1748 away from its exposed conformation to the position previously occupied by T1749. Thus, the deletion of K1750 results in the removal of at least two potential anchor points for negatively charged chemical groups in this region and may explain why the mutant shows decreased phosphatidyl inositol phosphate (PtdInsP) binding in overlay assays (D'Angelo, et al., 2006) (Supp. Figure S6). Such a peptide-flip could also explain a local increase in protein-flexibility suggested by thermal denaturation experiments, where the melting point was lowered (Supp. Figure S5). The mutation does not affect the content of bound lipids after exchange by incubation with liposomes of membrane like lipid composition, as demonstrated by mass spectrometry (Supp. Figure S1). Judging from the observed structural changes and their contribution to intramolecular contacts, we propose that the deletion would affect the interaction of the Sec14-PH module with potential ligands. Besides PtdInsPs also phosphoproteins or other species with local negative charge accumulations could be considered as such potential ligands in the cellular context. Since the PtdInsP binding site of full length neurofibromin is in overlay assays apparently accessible for ligands and displays a very similar binding profile with regard to the isolated Sec14-PH domain (A. Parret, unpublished observation), we consider it unlikely that the alteration affects extensive intramolecular interactions with neighboring domains. Taken together the structural analysis suggests that the

p.K1750del mutant is likely to interfere with protein-ligand interaction with the respective ligand yet to be established.

TD: The reported tandem duplication has been found in a patient displaying a heterogenous phenotype compatible with Watson- and Noonan-Syndrome (Tassabehji, et al., 1993) (MIM #193520 and #601321). Essentially, the linker peptide connecting the Sec14- and PH-like portions of neurofibromin is duplicated. The crystal structure shows the resulting segment (residues 1699' to 1712', Figure 1c; ' denotes duplicated residues) largely disordered with flanking regions slightly displaced and parts of the helical portion unwound. Despite the significant steric challenges imposed by the inserted peptide segment, the relative orientation of the two domains is rather similar to that observed in the wild-type situation. Given the presumably exposed arrangement of the lid-protrusion in the full length neurofibromin protein (A. Parret, unpublished observation), it is in fact likely that the linker region is exposed on the protein surface as well. Furthermore, the crystal structure points to a high flexibility of the duplicated linker, which is supported by thermal denaturation measurements showing unfolding at a significantly lower temperature compared with the wild type protein (Supp. Figure S5). Therefore the tandem duplication might not only block a potential protein binding site on the Sec14-PH module, but also reach and interfere with the surface or activities of spatial neighboring domains. Since protein-lipid overlay assays and lipid exchange experiments show results similar to that obtained with the wild type module, it is unlikely that the linker region blocks the lid-lock region or entry to the Sec14 lipid binding cage.

p.I1584V: The p.I1584V mutation is located in the hydrophobic core of the Sec14 domain on the backside of the lipid binding cage and is solvent shielded. As the

conservative removal of a single methyl group suggests, the wild-type and mutant protein structure look virtually identical (Figure 1e). Only a small difference of the protein backbone around the spatially close residue E1699 can be observed in one of the two molecules present in the crystal structure. This may indicate a local increase in flexibility which could alter the nearby surface region or have a different kinetic effect. Compared to the wild-type protein, the mutation does not interfere with lipid binding and exchange activities, indicating that the Sec14 cage as well as the lid-lock region remains undisturbed. With the present data we can only speculate that the subtle surface alterations interfere with a so far unidentified intra- or intermolecular protein-protein interaction surface. Taken together, our clinical and structural data suggests that p.I1584V is a functional mutation solely impairing a defined neurofibromin activity rather than disabling the functionality of the protein due to altered amounts, insolubility or instability.

Concluding Remarks

Patient-derived missense mutations can yield valuable insight into protein function and explain related consequences for cellular processes if they solely impair a defined activity. However, many mutations are reported on the DNA/RNA level, where it is not disclosed if this alteration prevents translation, is insoluble, unstable or indeed solely impairs a protein function. To discriminate between these cases, we verified the presence of wild-type-like neurofibromin levels in patient-derived cultured cells, if applicable, and expressed accordingly altered Sec14-PH constructs for biochemical analysis. Our results show the expression of p.K1750del and p.I1584V in patient-derived cultured cells and demonstrate that most recombinant constructs

are soluble and folded, supporting that these alterations have functional effects. Using X-ray crystallography of p.K1750del, p.I1584V and TD constructs we could furthermore identify and analyze the precise structural changes induced by these mutations. Whereas p.K1750del weakens the binding of negatively charged ligands to the PtdInsP binding site, the spatially close alteration TD introduces a bulky, flexible insertion while p.I1584V seems to affect a surface patch in the proximity to this region. Since ~~the different~~ most alterations do not disturb ~~the lipid~~ binding of PtdInsP to the domain interface region (Supp. Figure S6) or the glycerophospholipid exchange activity of the Sec14 cage (Supp. Figure S1), we suggest that a so far unknown ligand binding activity involving the lid-lock region is impaired, consistent with the structural effects of p.K1750del and its reduced capability to bind PtdInsP. Taking into account that the lid-lock region appears to be accessible in the full length protein (A. Parret, unpublished observation), we would expect an intermolecular contact surface in this area. As potential ligands, certain phosphoproteins or similar species with strong local negative charges could be imagined besides PtdInsPs. Taken together, our study highlights mutations in the Sec14-PH module as likely modifiers of important structural regions of neurofibromin that may affect protein-protein interaction on a physiological level. Furthermore it suggests that the non-truncating mutations of the Sec14-PH module do not have a major effect on the lipid binding properties of the Sec14 lipid binding cage.

Protein Data Bank (PDB) accession codes: The coordinates for the analyzed mutations of human HsNF1 Sec14-PH were deposited in the RCSB Protein Data Bank with the accession codes XXXX (p.K1750del), XXXX (TD) and XXXX (p.I1584V).

Acknowledgement: We thank F. Bonneau for expert technical assistance, U. Karst for investigating initial crystallization of p.K1750del mutant, the staff at ESRF for technical support with X-ray data collection. This work was supported by the US Department of Defense (DAMD17-00-1-0539) and the “Proteinbiochemistry / Proteomics” research program of the Baden-Württemberg Stiftung, Germany.

Bibliography

Adams PD, Grosse-Kunstleve RW, Hung LW, Ioerger TR, McCoy AJ, Moriarty NW, Read RJ, Sacchettini JC, Sauter NK, Terwilliger TC. 2002. PHENIX: building new software for automated crystallographic structure determination. Acta Crystallogr D Biol Crystallogr 58(Pt 11):1948-54.

Bonneau F, D'Angelo I, Welti S, Stier G, Ylanne J, Scheffzek K. 2004. Expression, purification and preliminary crystallographic characterization of a novel segment from the neurofibromatosis type 1 protein. Acta Crystallogr D Biol Crystallogr 60(Pt 12 Pt 2):2364-7.

Boyanapalli M, Lahoud OB, Messiaen L, Kim B, Anderle de Sylor MS, Duckett SJ, Somara S, Mikol DD. 2006. Neurofibromin binds to caveolin-1 and regulates ras, FAK, and Akt. Biochem Biophys Res Commun 340(4):1200-8.

Brugger B, Glass B, Haberkant P, Leibrecht I, Wieland FT, Krausslich HG. 2006. The HIV lipidome: a raft with an unusual composition. Proc Natl Acad Sci U S A 103(8):2641-6.

Brunger AT, Adams PD, Clore GM, DeLano WL, Gros P, Grosse-Kunstleve RW, Jiang JS, Kuszewski J, Nilges M, Pannu NS and others. 1998. Crystallography & NMR system: A new software suite for macromolecular structure determination. Acta Crystallogr D Biol Crystallogr 54(Pt 5):905-21.

Calderon RO, DeVries GH. 1997. Lipid composition and phospholipid asymmetry of membranes from a Schwann cell line. J Neurosci Res 49(3):372-80.

CCP4. 1994. The CCP4 suite: programs for protein crystallography. Acta Crystallogr D Biol Crystallogr 50(Pt 5):760-3.

Cichowski K, Jacks T. 2001. NF1 tumor suppressor gene function: narrowing the GAP. Cell 104(4):593-604.

D'Angelo I, Welti S, Bonneau F, Scheffzek K. 2006. A novel bipartite phospholipid-binding module in the neurofibromatosis type 1 protein. EMBO Rep 7(2):174-9.

Emsley P, Cowtan K. 2004. Coot: model-building tools for molecular graphics. Acta Crystallogr D Biol Crystallogr 60(Pt 12 Pt 1):2126-32.

Fahsold R, Hoffmeyer S, Mischung C, Gille C, Ehlers C, Kucukceylan N, Abdel-Nour M, Gewies A, Peters H, Kaufmann D and others. 2000. Minor lesion mutational spectrum of the entire NF1 gene does not explain its high mutability but points to a functional domain upstream of the GAP-related domain. Am J Hum Genet 66(3):790-818.

Griesser J, Kaufmann D, Maier B, Mailhammer R, Kuehl P, Krone W. 1997. Post-transcriptional regulation of neurofibromin level in cultured human melanocytes in response to growth factors. J Invest Dermatol 108(3):275-80.

Griffiths S, Thompson P, Frayling I, Upadhyaya M. 2007. Molecular diagnosis of neurofibromatosis type 1: 2 years experience. Fam Cancer 6(1):21-34.

Han SS, Cooper DN, Upadhyaya MN. 2001. Evaluation of denaturing high performance liquid chromatography (DHPLC) for the mutational analysis of the neurofibromatosis type 1 (NF1) gene. Hum Genet 109(5):487-97.

Izawa I, Tamaki N, Saya H. 1996. Phosphorylation of neurofibromatosis type 1 gene product (neurofibromin) by cAMP-dependent protein kinase. FEBS Lett 382(1-2):53-9.

Jeong SY, Park SJ, Kim HJ. 2006. The spectrum of NF1 mutations in Korean patients with neurofibromatosis type 1. J Korean Med Sci 21(1):107-12.

Kabsch W. 1993. Automatic Processing of Rotation Diffraction Data from Crystals of

Initially Unknown Symmetry and Cell Constants. J. Appl. Cryst. 26:795-800.
Kaufmann D, Bartelt B, Hoffmeyer S, Muller R. 1999a. Posttranslational regulation of neurofibromin content in melanocytes of neurofibromatosis type 1 patients. Arch Dermatol Res 291(6):312-7.
Kaufmann D, Gruener S, Braun F, Stark M, Griesser J, Hoffmeyer S, Bartelt B. 1999b. EVI2B, a gene lying in an intron of the neurofibromatosis type 1 (NF1) gene, is as the NF1 gene involved in differentiation of melanocytes and keratinocytes and is overexpressed in cells derived from NF1 neurofibromas. DNA Cell Biol 18(5):345-56.
Klose A, Ahmadian MR, Schuelke M, Scheffzek K, Hoffmeyer S, Gewies A, Schmitz F, Kaufmann D, Peters H, Wittinghofer A and others. 1998. Selective disactivation of neurofibromin GAP activity in neurofibromatosis type 1. Hum Mol Genet 7(8):1261-8.
Le LQ, Parada LF. 2007. Tumor microenvironment and neurofibromatosis type I: connecting the GAPs. Oncogene 26(32):4609-16.
Lee MJ, Su YN, You HL, Chiou SC, Lin LC, Yang CC, Lee WC, Hwu WL, Hsieh FJ, Stephenson DA and others. 2006. Identification of forty-five novel and twenty-three known NF1 mutations in Chinese patients with neurofibromatosis type 1. Hum Mutat 27(8):832.
McClatchey AI, Cichowski K. 2001. Mouse models of neurofibromatosis. Biochim Biophys Acta 1471(2):M73-80.
Murshudov GN, Vagin AA, Dodson EJ. 1997. Refinement of macromolecular structures by the maximum-likelihood method. Acta Crystallogr D Biol Crystallogr 53(Pt 3):240-55.
Painter J, Merritt EA. 2006. Optimal description of a protein structure in terms of multiple groups undergoing TLS motion. Acta Crystallogr D Biol Crystallogr 62(Pt 4):439-50.
Painter JaM, A. 2006. TLSMD web server for the generation ofmulti-group TLSmodels. Applied Crystallography 39:109-111.
Patrakitkomjorn S, Kobayashi D, Morikawa T, Wilson MM, Tsubota N, Irie A, Ozawa T, Aoki M, Arimura N, Kaibuchi K and others. 2008. Neurofibromatosis type 1 (NF1) tumor suppressor, neurofibromin, regulates the neuronal differentiation of PC12 cells via its associating protein, CRMP-2. J Biol Chem 283(14):9399-413.
Phan VT, Ding VW, Li F, Chalkley RJ, Burlingame A, McCormick F. 2010. The RasGAP proteins Ira2 and neurofibromin are negatively regulated by Gpb1 in yeast and ETEA in humans. Mol Cell Biol 30(9):2264-79.
Riccardi VM. 1992. Neurofibromatosis: Phenotype Natural History, and Pathogenesis, Second Edition (Baltimore and London: The Johns Hopkins University Press.
Sambrook J, Russell DW. 2001. Molecular Cloning. Cold Spring Harbor: Cold Spring Harbor Laboratory Press.
Scheffzek K, Ahmadian MR, Wiesmuller L, Kabsch W, Stege P, Schmitz F, Wittinghofer A. 1998. Structural analysis of the GAP-related domain from neurofibromin and its implications. Embo J 17(15):4313-27.
Shen MH, Harper PS, Upadhyaya M. 1996. Molecular genetics of neurofibromatosis type 1 (NF1). J Med Genet 33(1):2-17.
Tassabehji M, Strachan T, Sharland M, Colley A, Donnai D, Harris R, Thakker N. 1993. Tandem duplication within a neurofibromatosis type 1 (NF1) gene exon in a family with features of Watson syndrome and Noonan syndrome. Am J

Hum Genet 53(1):90-5.
Upadhyaya M, Cooper DN. 1998. Neurofibromatosis Type 1 from genotype to phenotype.
Upadhyaya M, Maynard J, Osborn M, Harper PS. 1997. Six novel mutations in the neurofibromatosis type 1 (NF1) gene. Hum Mutat 10(3):248-50.
Viskochil D, White R, Cawthon R. 1993. The neurofibromatosis type 1 gene. Annu Rev Neurosci 16:183-205.
Welti S, D'Angelo I, Scheffzek K. 2008. Structure and Function of Neurofibromin. Monogr Hum Genet 16:113-128.
Welti S, Fraterman S, D'Angelo I, Wilm M, Scheffzek K. 2007. The sec14 homology module of neurofibromin binds cellular glycerophospholipids: mass spectrometry and structure of a lipid complex. J Mol Biol 366(2):551-62.
Wu R, Lopez-Correa C, Rutkowski JL, Baumbach LL, Glover TW, Legius E. 1999. Germline mutations in NF1 patients with malignancies. Genes Chromosomes Cancer 26(4):376-80.
Zhu Y, Parada LF. 2001. Neurofibromin, a tumor suppressor in the nervous system. Exp Cell Res 264(1):19-28.

Figure. 1: Structural changes induced by patient-derived mutations
a) Domain scheme of neurofibromin (2818aa) showing the Sec14, pleckstrin homology (PH) like, cystein and serine rich- (CSRD) and GAP related domain (GRD). Domains are drawn to scale. **b)** Structure of the wild-type Sec14-PH domains of neurofibromin with positions where selected patient-derived alterations have been observed highlighted in yellow. **c)** Superposition of TD (green) with the wild-type protein (red/yellow/violet). The overall fold and orientation of the Sec14 and PH domains is conserved. In the mutant structure, the linker region is not visible (green dashed line), indicating a high flexibility of the region. A ‘ denotes duplicated residues. **d)** p.K1750del induces a structural rearrangement in the “lock” region. The wild-type structure is shown in red, p.K1750del in orange. R1748 is flipped to the former position of T1749, which is now oriented like the deleted K1750. Therewith, K1750 and R1748 are no longer available for ligand binding. **e)** Superposition of the p.I1584V (green) and wild-type (violet) structure. Mutant and wild-type structures show virtually no differences apart from the p.I1584V amino acid substitution, which is well defined in the electron density map (orange).

Figure 2:. Determination of neurofibromin content in the NF1 patients. Normal neurofibromin levels were found in NF1- p.K1750del and NF1-p.I1584V as compared with healthy donors (K1, K2 and K3). Reduced neurofibromin levels were detected in NF1 patients with truncating mutations (NF71, NF10 and NF106 (Kaufmann, et al., 1999b)). Neurofibromin content was measured in peripheral blood cells by immunoprecipitation and Western blotting as described (Griesser, et al., 1997; Klose, et al., 1998) .

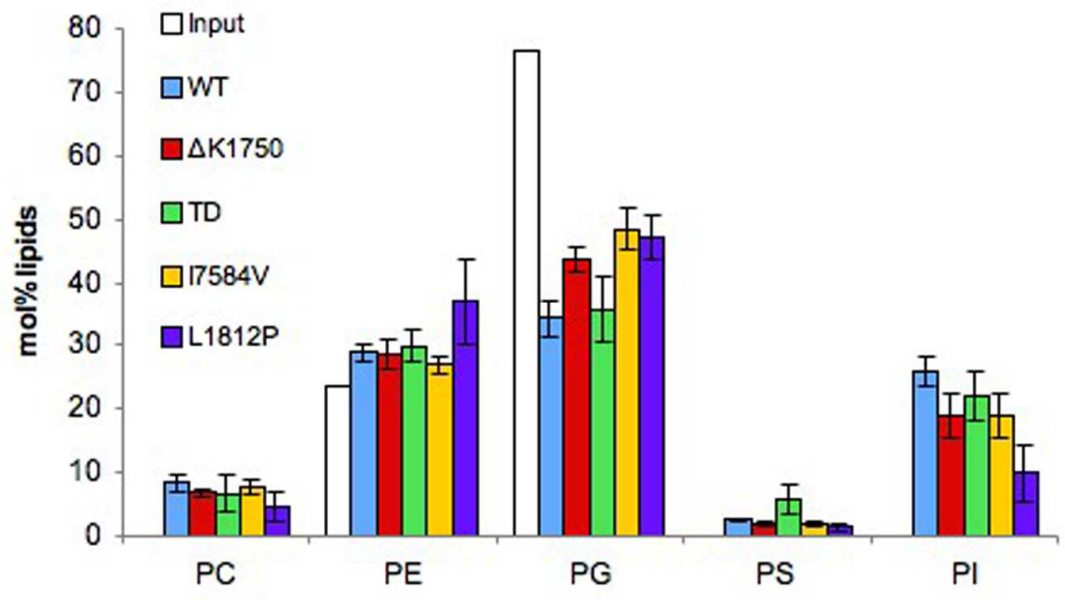

Supplementary Figure S1:

Lipid profiles of wild-type NF1 Sec14-PH and selected representative mutants. Following liposomal exchange assays, proteins were subjected to quantitative lipid analysis by nano-mass spectrometry. Data are the mean ± margin of deviation of three different experiments; for input values n =1. "Input" corresponds to the lipid content of the wild-type NF1 Sec14-PH protein prior to lipid exchange.

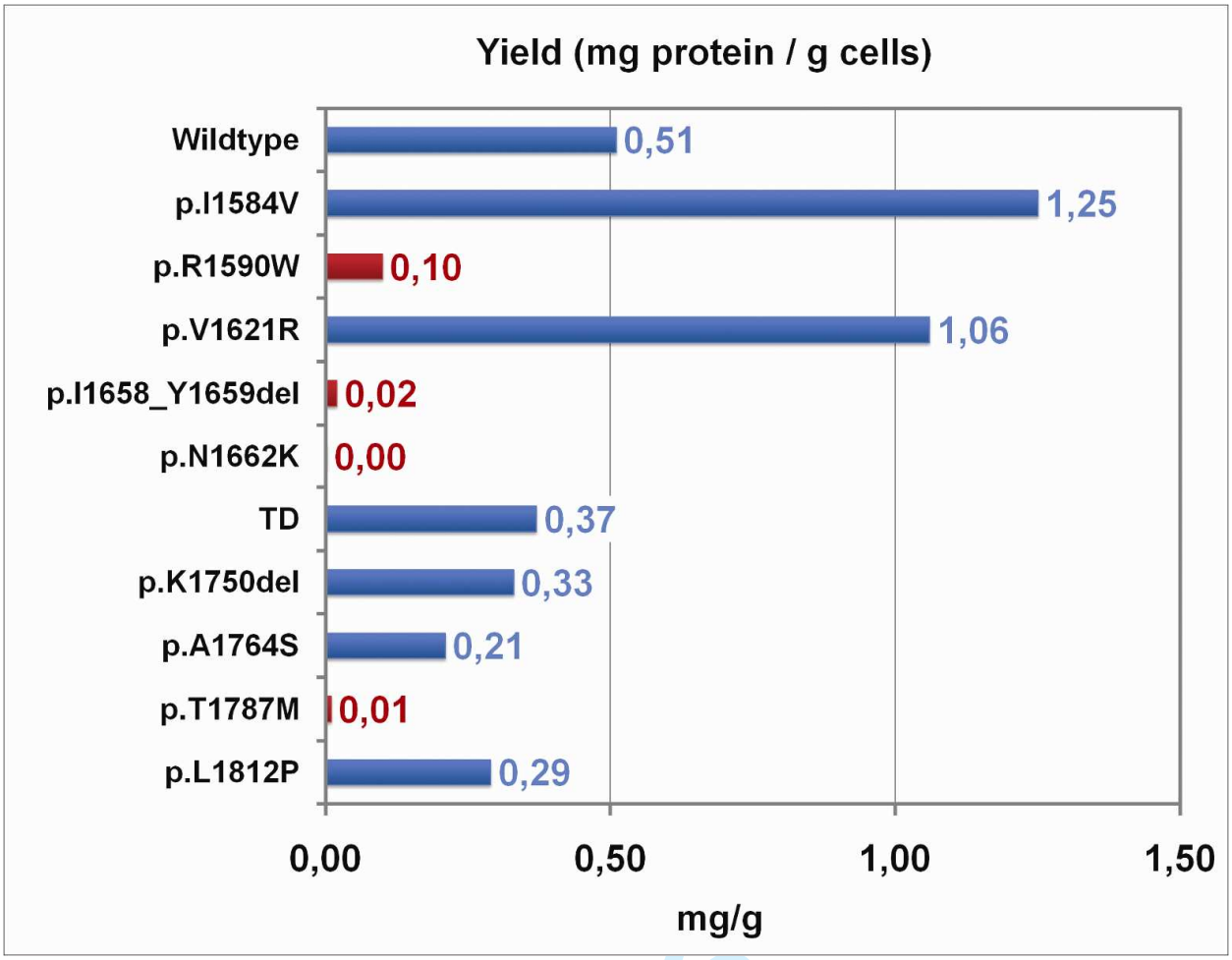

Supplementary Figure S2: Protein yield of the different mutant Sec14-PH proteins compared to the wild-type protein. Red bars indicate that the protein was not further analyzed.

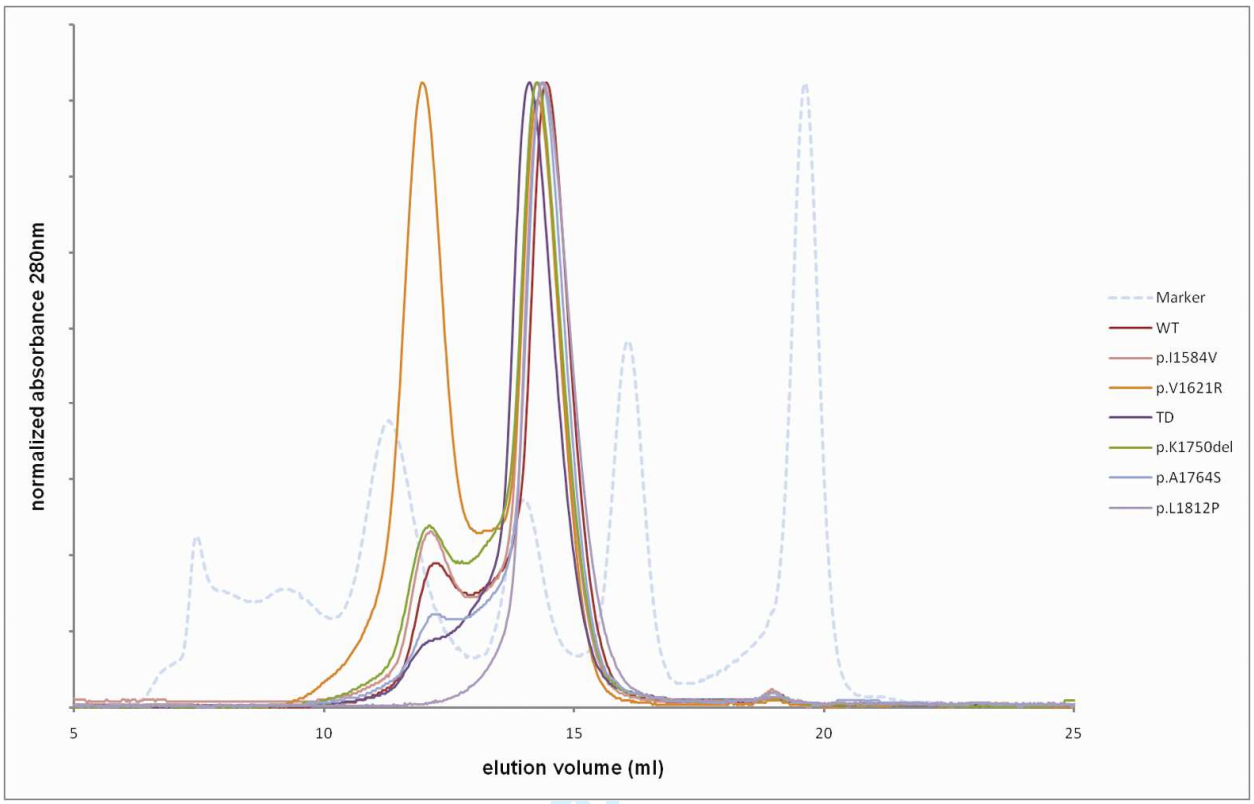

Supplementary Figure S3:

Analytical size exclusion chromatograms of Sec14-PH and the analyzed patient-derived mutations. All proteins are present in a monomer – dimer equilibrium, with the majority of protein present as monomer (peak near 15ml). p.V1621R seems to have an elevated fraction of dimeric protein under these conditions.

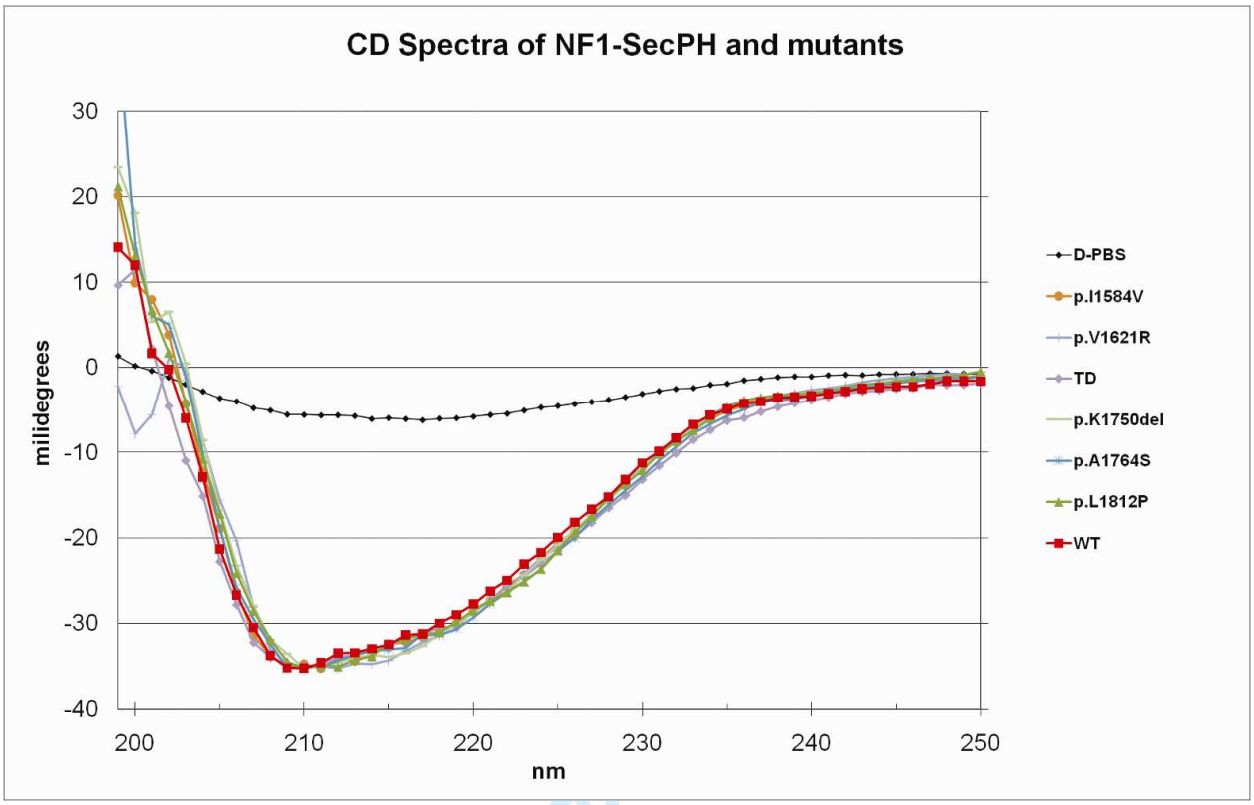

Supplementary Figure S4: CD analysis

CD spectra of the wild-type NF1 Sec14-PH protein and the analyzed mutant constructs. Despite different alterations, the overall folds of the mutated constructs are not impaired.

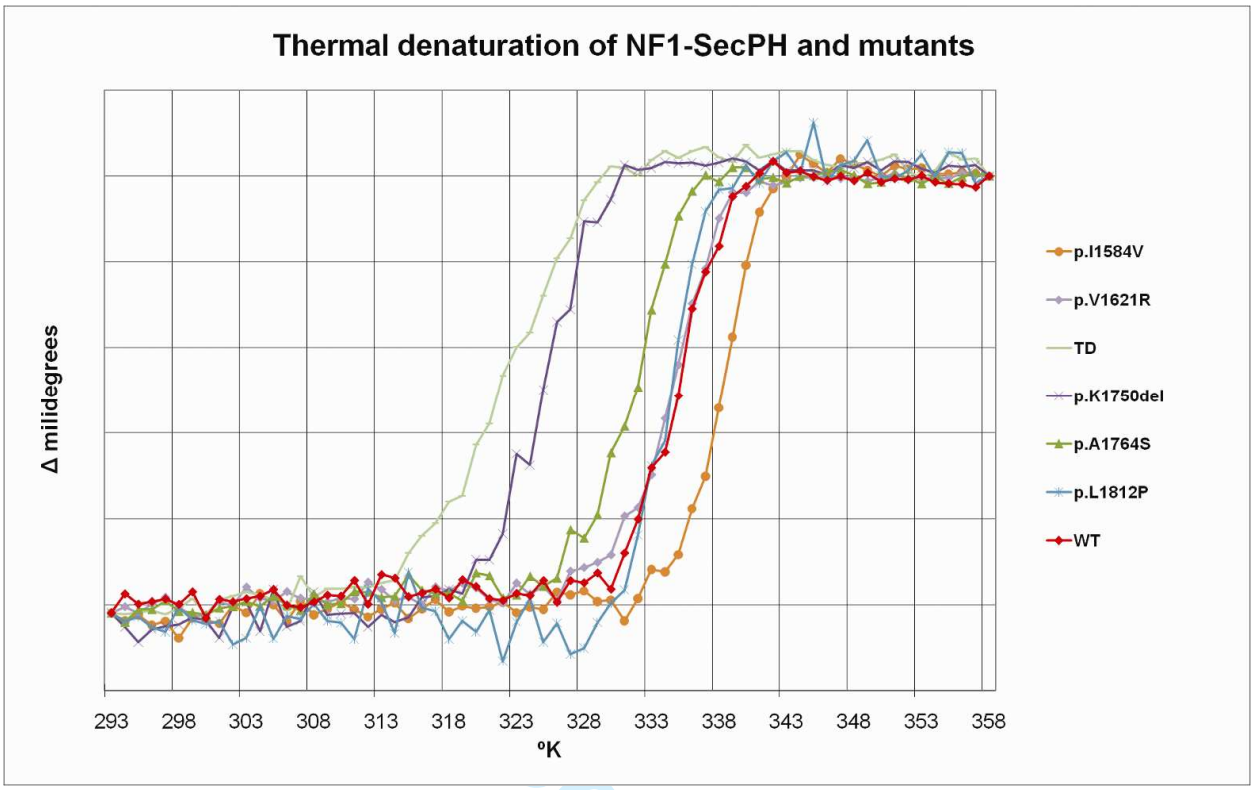

Supplementary Figure S5: CD thermal denaturation analysis

Melting curves of the wild-type NF1 Sec14-PH and the mutant constructs. Most constructs including the wild-type, show a melting temperature around 60-65℃. The TD and p.K1750del alterations show a significantly reduced melting temperature around 50-53℃, indicating an increased flexibility of these mutants.

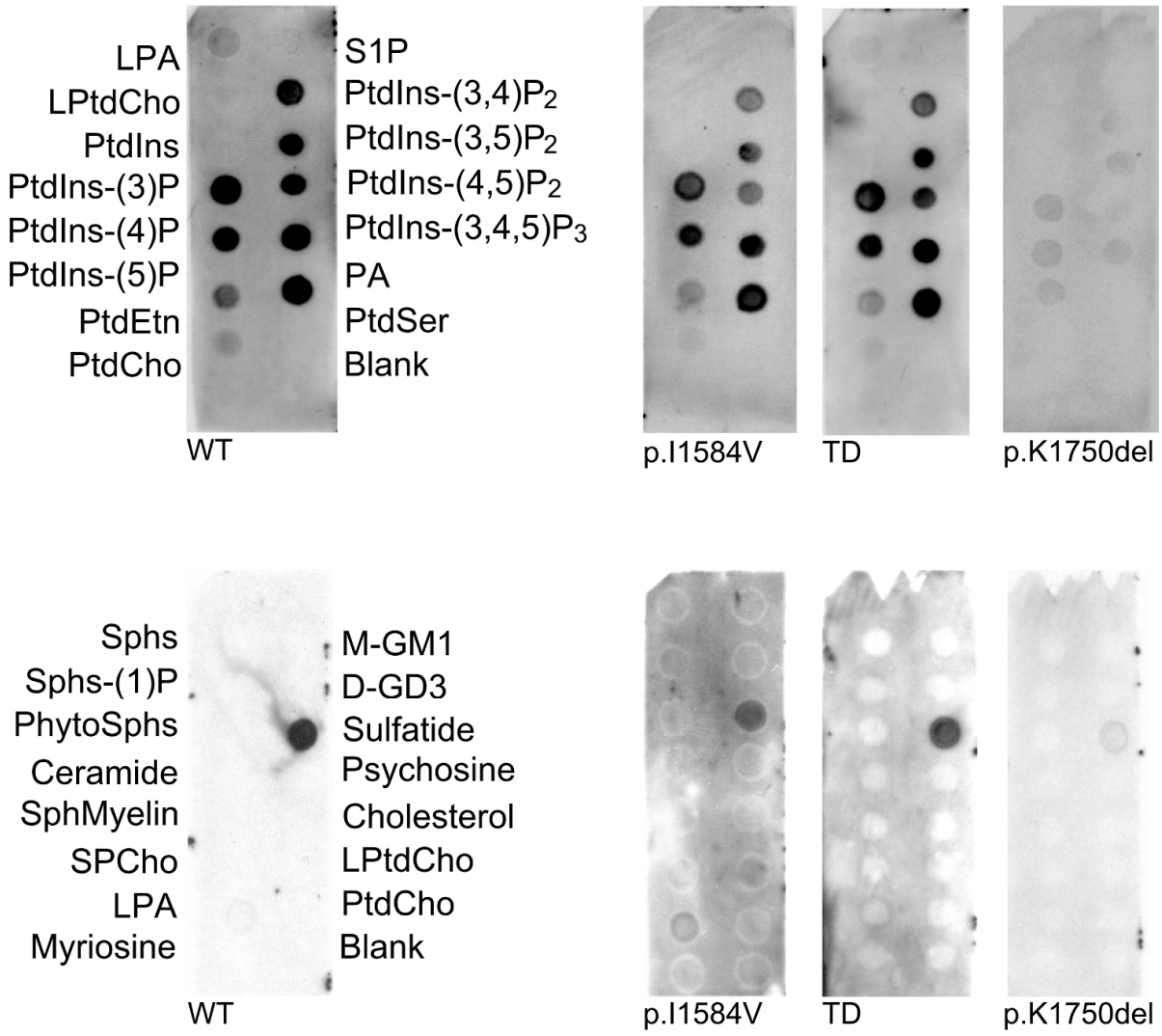

Supplementary Figure S6:

Protein – lipid overlay assays with the wild-type NF1 Sec14-PH construct and selected representative mutants. The mutants which are not displayed, show a similar binding pattern like the wild-type protein. For p.K1750del a reduced signal can be observed which is consistent with the effect of the alteration to the PtdInsP binding platform (see text).

Supplementary Table S1 Primers PCR primers for the generation of the tandem duplication TD mutant construct

TD-5'fwd	TATATCCATGGGCAGTTCAAAGTTTGAGGAATTTATGACTAGG	NcoI
TD-5'rev	TATATGGTCTCGTAGTTTCTGTTGTTCATGCCCTAAAGCCAAGGTGGCAGC	BsaI
TD-3'fwd	TATATGGTCTCAACTACCTGCTGCCACCTTGGCTTTAGAAGAGGACCTGAAGGTA	BsaI
TD-3'rev	ATACATTTATGCGGCCGCTAGTCGGGCTGTGACAGTTCCCAGCGGGTCC	NotI

Table 1: Overview of patient-derived mutations in the Sec14-PH region of neurofibromin and summary of results.

Mutation	yield, solubility	GF	CD	T_M	X-ray analysis	cultured cells
c.4750A>G (p.I1584V) (Fahsold, et al., 2000)	+	+	+	as wt	structure	present
c.4768C>T (p.R1590W) (Upadhyaya, et al., 1997)	-					
c.4861_4862delinsAG (p.V1621R) (Jeong, et al., 2006)	+	+	+	as wt		
c.4973_4978delTCTATA (p.I1658_Y1659del) (Wu, et al., 1999)	-					
p.N1662K (Boyanapalli, et al., 2006)	-					
c.5136_5137insGGGCATGAACAACAGAAACTACCTGCTGCCACCTTGGCTTTA (p.L1713_E1714insGHEQQKLPAATLAL) "tandem duplication (TD)" (Tassabehji, et al., 1993)	+	+	+	lower	structure	
c.5248_5250delAAA (p.K1750del) (Fahsold, et al., 2000)	+	+	+	lower	structure	present
c.5290G>T (p.A1764S) (Han, et al., 2001)	+	+	+	as wt		
c.5360C>G (p.T1787M) (Lee, et al., 2006)	-					
c.5435T>C (p.R1812P) (Griffiths, et al., 2007)	+	+	+	as wt		

GF: gelfiltration, CD: circular dicroism, TM: melting temperature in thermal denaturation experiments, cultured cells: presence of neurofibromin in patient-

derived cultured cells. Nucleotide and codon numbering is based on the cDNA reference sequence. Codon 1 is the initiation codon ATG with the Nucleotides +1 to +3, according to journal guidelines (www.hgvs.org/mutnome).

Table 2 Crystallization, X-ray data collection and structure refinement

Data collection	**NF1 Sec14-PH-p.K1750del**	**NF1 SecPH-TD**	**NF1 SecPH-PH-p.I1584V**
X-ray source	ESRF Grenoble ID14-1	ESRF Grenoble ID14-3	ESRF Grenoble ID 29
Wavelength [Å]	0.934	0.931	0.979
Space group	P4(1)2(1)2	P6(4)22	P4(1)2(1)2
Unit cell a,b,c [Å] α,β,γ [deg]	113.4/113.4/124.5 90/90/90	104.6/104.6/116.3 90/90/120	113.1/113.1/124.6 90/90/90
Resolution [Å]	2.2	2.52	2.65
Highest shell	2.2-2.31	2.52 – 2.67	2.65 – 2.80
No. of observations	270,047 (36,483)	300,107 (10,519)	229,751 (35,000)
Unique reflections	42,265 (6,055)	12,507 (1,532)	24,098 (3,584)
I/σ	13.9 (3.8)	21.78 (2.49)	23.02 (3.51)
R_{meas} [%]*	7.3 (49.1)	11.2 (78.4)	9.0 (83.1)
Completeness [%]	99.6 (99.5)	94.5 (75.4)	99.9 (99.9)
Refinement			
Resolution range [Å]	19.95 – 2.25	19.57 – 2.52	49 – 2.65
No. of reflections	39,869	11,879	24,081
R_{work}/R_{free}†	0.208 / 0.249	0.223 / 0.264	0.216 / 0.266
No. of atoms Protein	4,011	1,963	4,373
No. of atoms Solvent	241	36	166
No. of atoms Ligands	110	47	117
RMSD Bond length [Å] Bond angle [deg]	 0.004 0.90	 0.003 0.61	 0.002 0.54
PDB accession code	XXXX	XXXX	XXXX

* as defined in XDS (Kabsch, 1993). † as defined in Phenix (Adams, et al., 2002). Numbers in brackets indicate values for the highest shell.

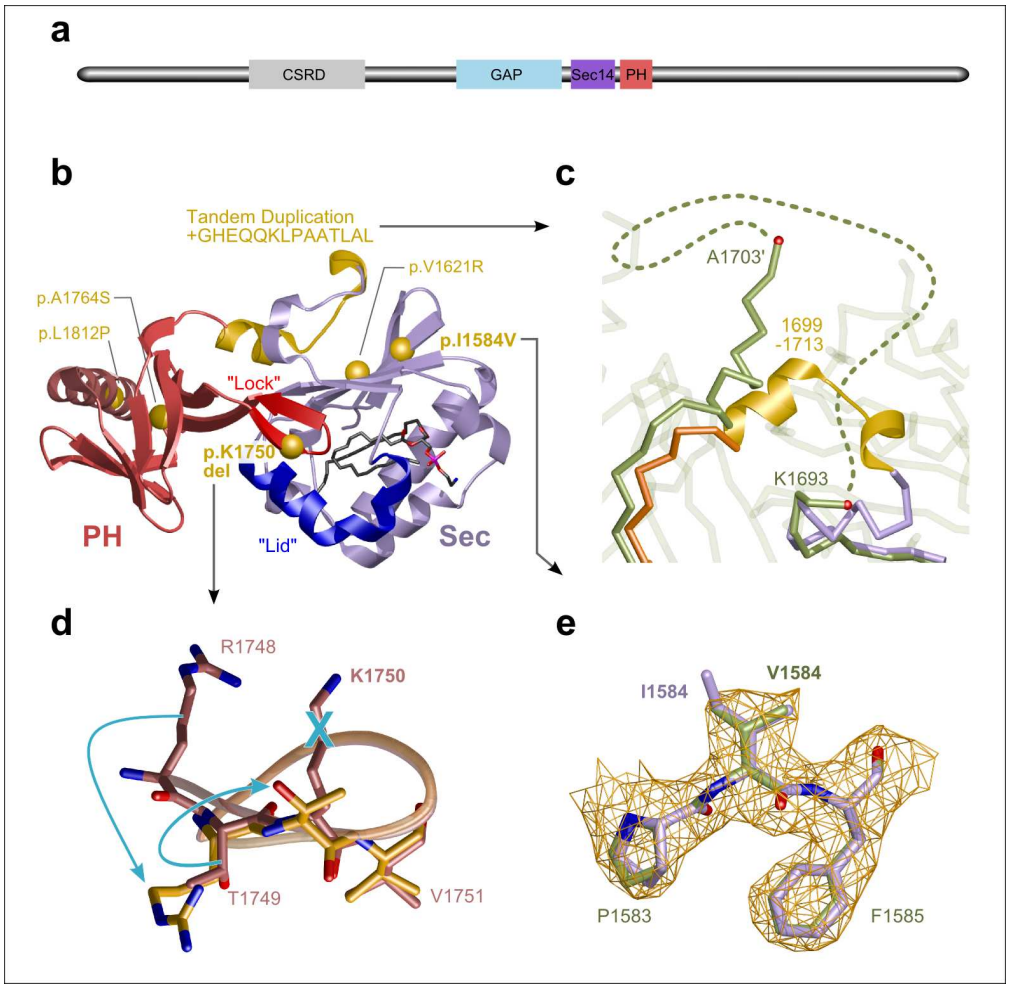

Figure. 1: Structural changes induced by patient-derived mutations
a) Domain scheme of neurofibromin (2818aa) showing the Sec14, pleckstrin homology (PH) like, cystein and serine rich- (CSRD) and GAP related domain (GRD). Domains are drawn to scale. b) Structure of the wild-type Sec14-PH domains of neurofibromin with positions where selected patient-derived alterations have been observed highlighted in yellow. c) Superposition of TD (green) with the wild-type protein (red/yellow/violet). The overall fold and orientation of the Sec14 and PH domains is conserved. In the mutant structure, the linker region is not visible (green dashed line), indicating a high flexibility of the region. A ' denotes duplicated residues. d) p.K1750del induces a structural rearrangement in the "lock" region. The wild-type structure is shown in red, p.K1750del in orange. R1748 is flipped to the former position of T1749, which is now oriented like the deleted K1750. Therewith, K1750 and R1748 are no longer available for ligand binding. e) Superposition of the p.I1584V (green) and wild-type (violet) structure. Mutant and wild-type structures show virtually no differences apart from the p.I1584V amino acid substitution, which is well defined in the electron density map (orange).

540x529mm (74 x 74 DPI)

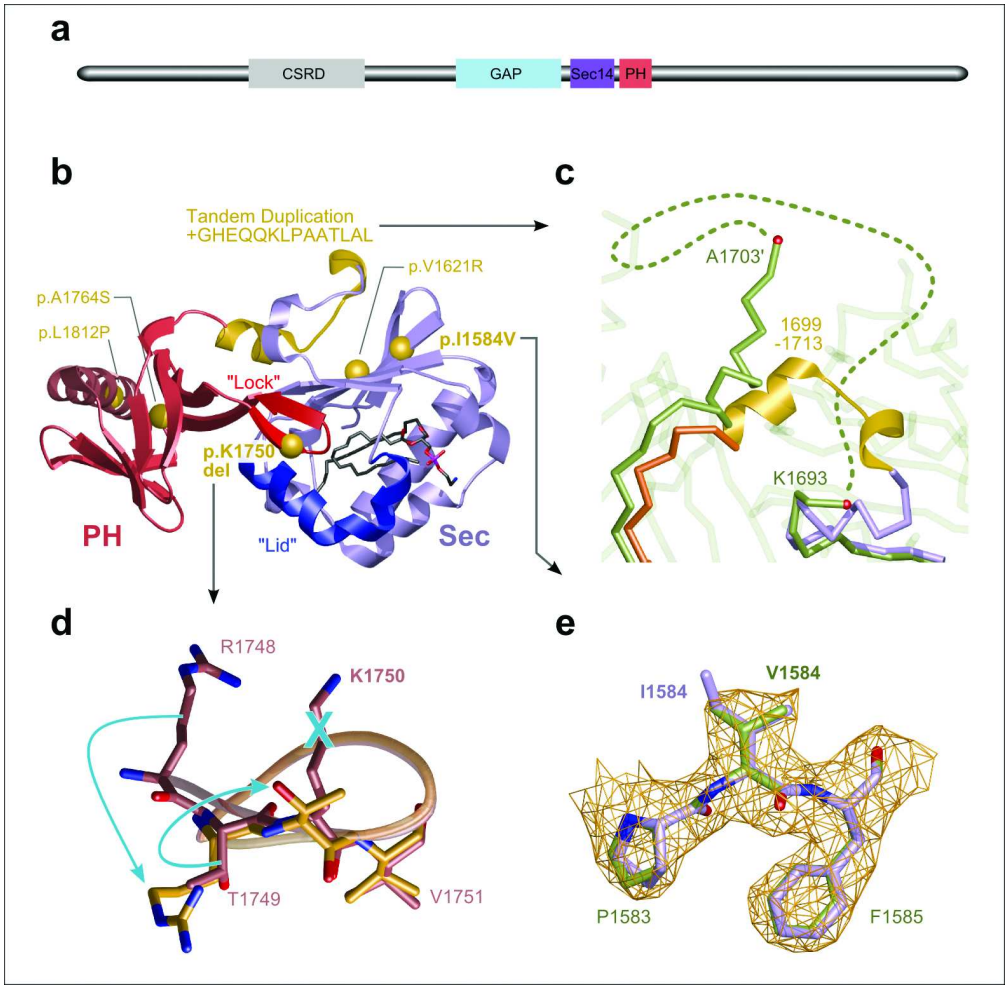

540x529mm (74 x 74 DPI)

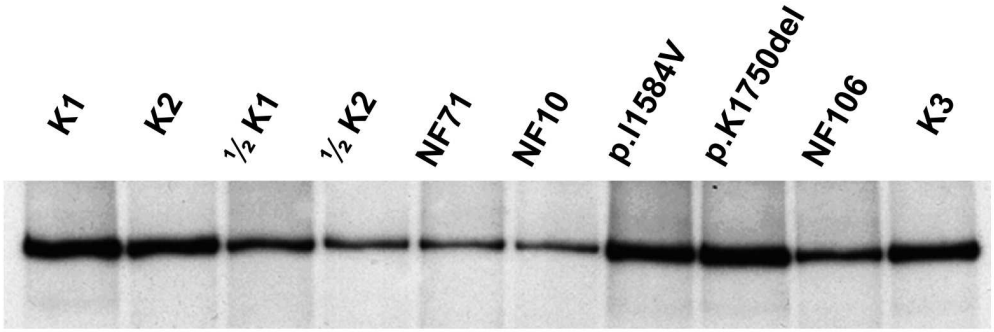

Figure 2:. Determination of neurofibromin content in the NF1 patients. Normal neurofibromin levels were found in NF1- p.K1750del and NF1-p.I1584V as compared with healthy donors (K1, K2 and K3). Reduced neurofibromin levels were detected in NF1 patients with truncating mutations (NF71, NF10 and NF106 (Kaufmann, et al., 1999b)). Neurofibromin content was measured in peripheral blood cells by immunoprecipitation and Western blotting as described (Griesser, et al., 1997; Klose, et al., 1998) .
200x68mm (200 x 200 DPI)

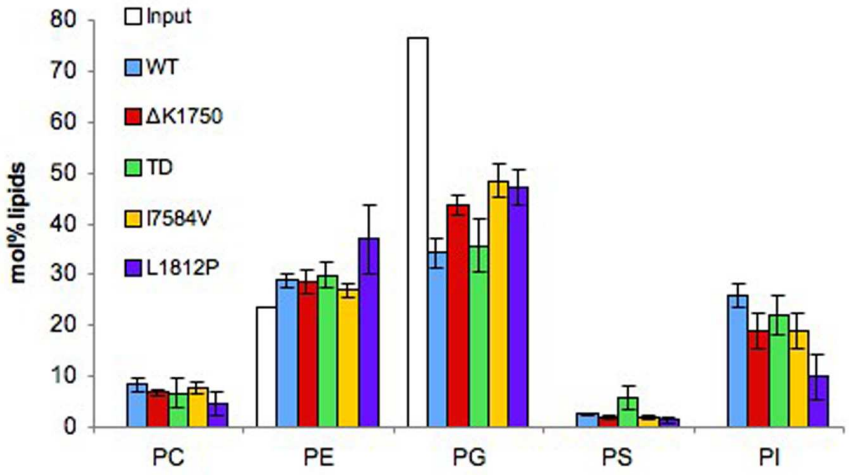

Supplementary Figure S1:
Lipid profiles of wild-type NF1 Sec14-PH and selected representative mutants. Following liposomal exchange assays, proteins were subjected to quantitative lipid analysis by nano-mass spectrometry. Data are the mean ± margin of deviation of three different experiments; for input values n =1. "Input" corresponds to the lipid content of the wild-type NF1 Sec14-PH protein prior to lipid exchange.

66x34mm (600 x 600 DPI)

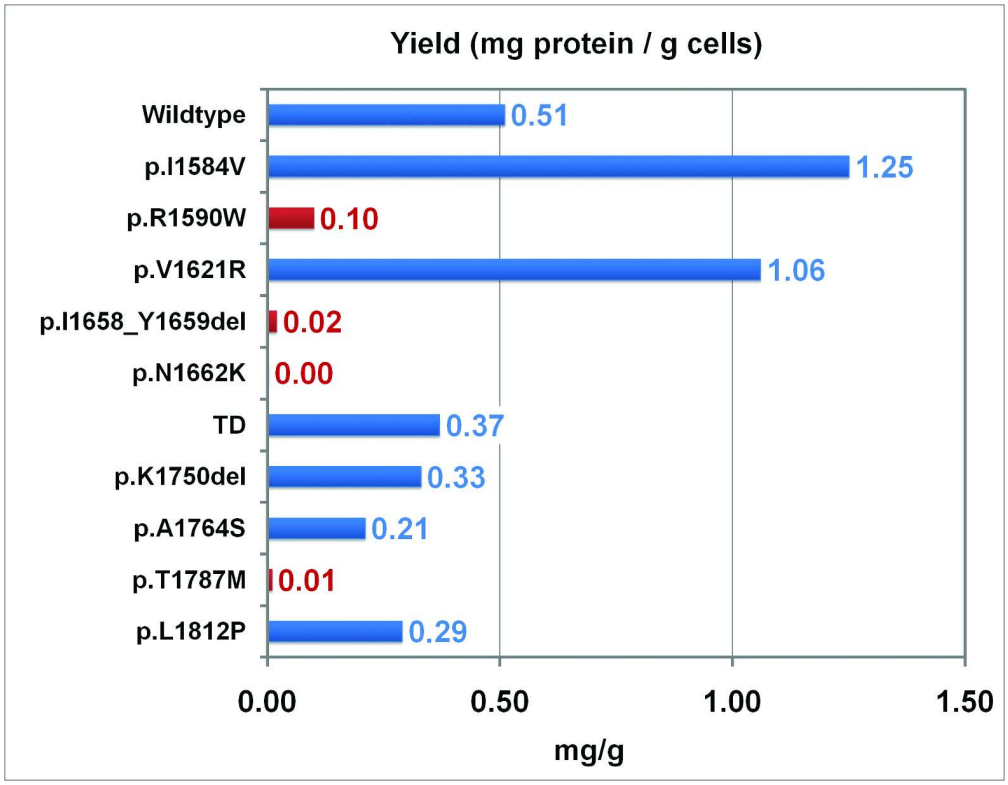

Supplementary Figure S2: Protein yield of the different mutant Sec14-PH proteins compared to the wild-type protein. Red bars indicate that the protein was not further analyzed.
200x155mm (200 x 200 DPI)

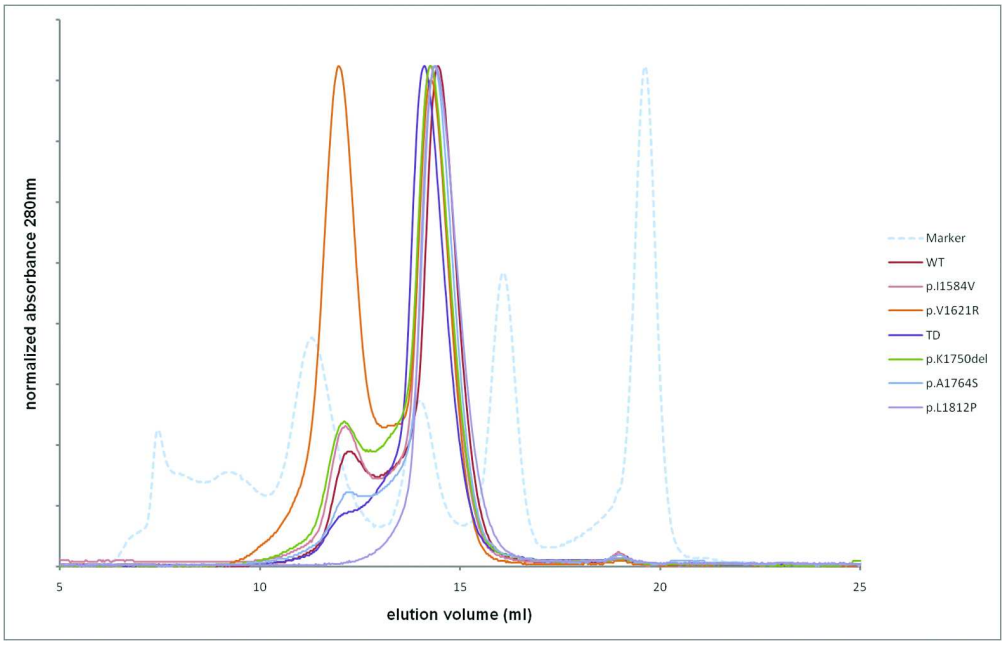

Supplementary Figure S3:
Analytical size exclusion chromatograms of Sec14-PH and the analyzed patient-derived mutations. All proteins are present in a monomer – dimer equilibrium, with the majority of protein present as monomer (peak near 15ml). p.V1621R seems to have an elevated fraction of dimeric protein under these conditions.

200x127mm (200 x 200 DPI)

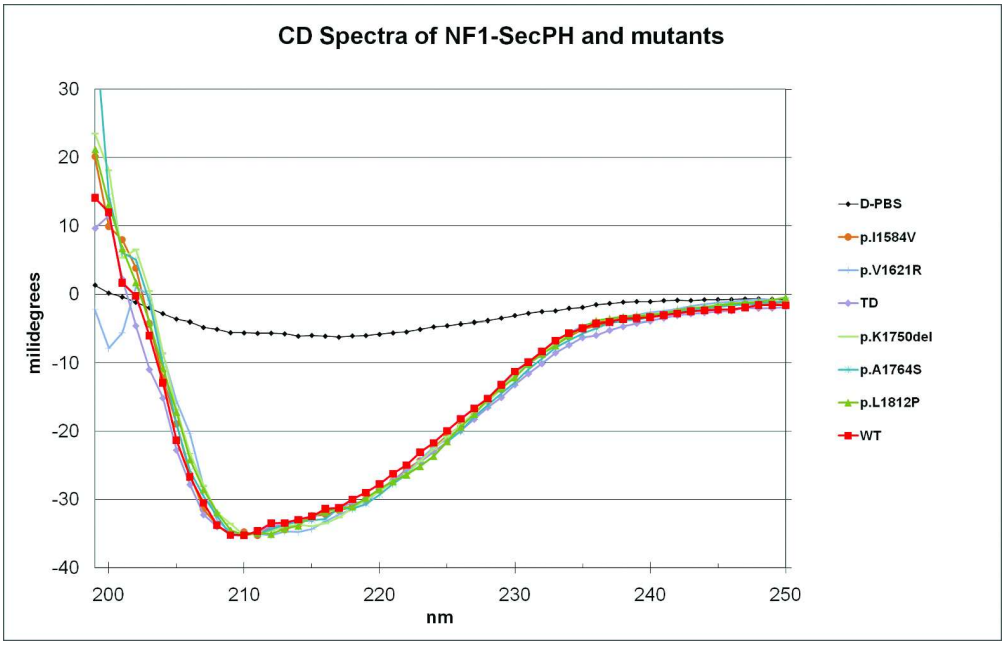

Supplementary Figure S4: CD analysis
CD spectra of the wild-type NF1 Sec14-PH protein and the analyzed mutant constructs. Despite different alterations, the overall folds of the mutated constructs are not impaired.

200x127mm (200 x 200 DPI)

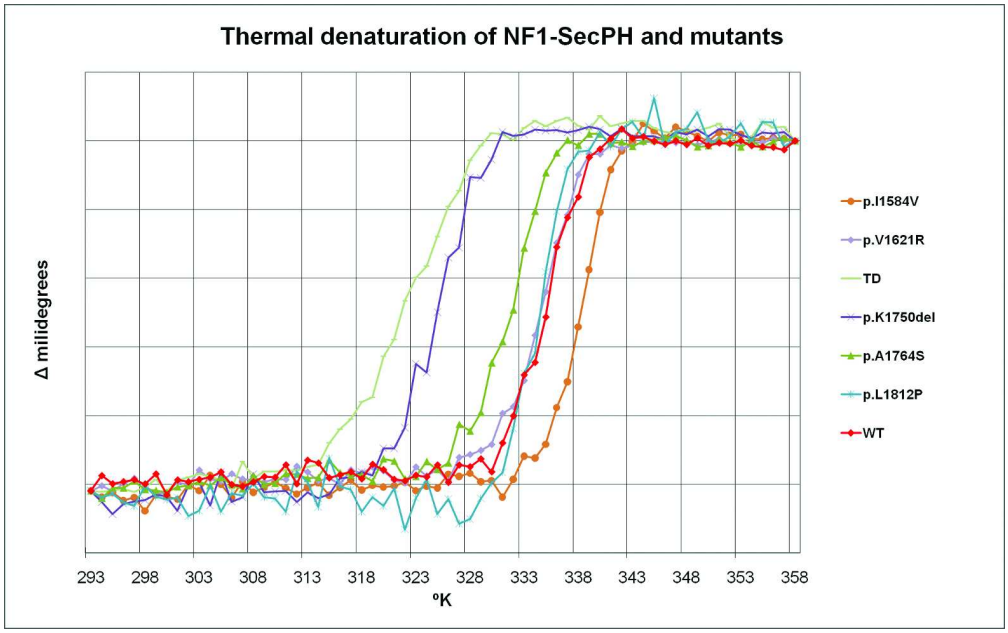

Supplementary Figure S5: CD thermal denaturation analysis
Melting curves of the wild-type NF1 Sec14-PH and the mutant constructs. Most constructs including the wild-type, show a melting temperature around 60-65°C. The TD and p.K1750del alterations show a significantly reduced melting temperature around 50-53°C, indicating an increased flexibility of these mutants.

200x125mm (200 x 200 DPI)

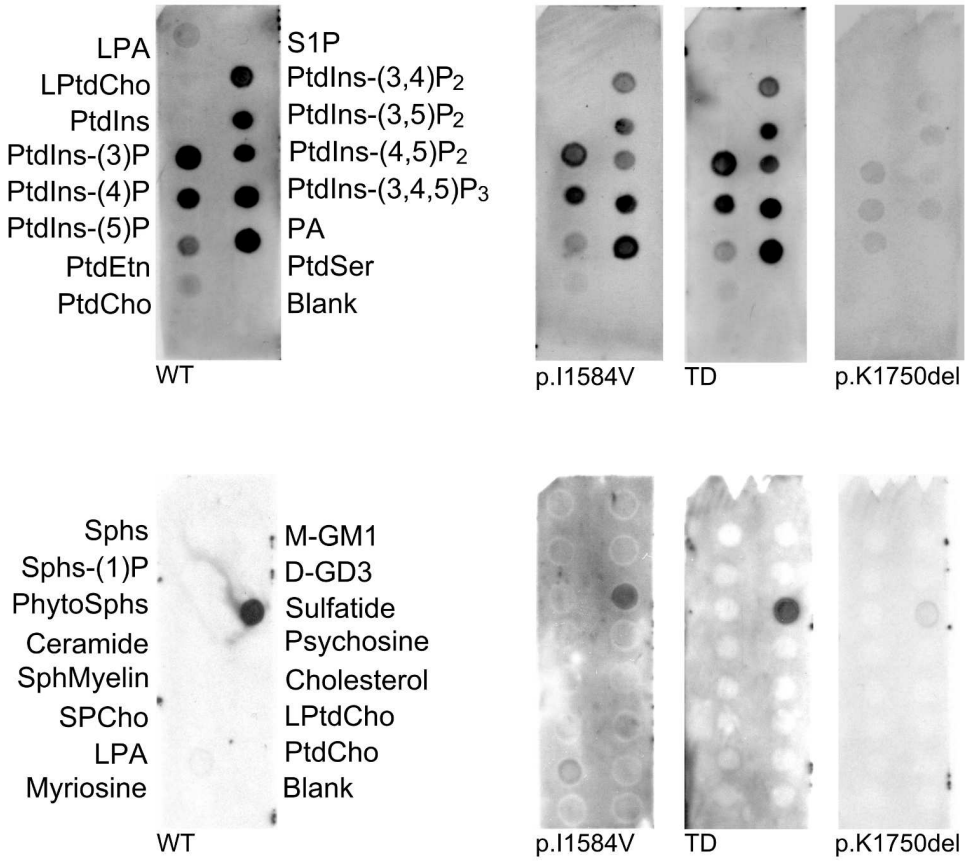

Supplementary Figure S6:
Protein – lipid overlay assays with the wild-type NF1 Sec14-PH construct and selected representative mutants. The mutants which are not displayed, show a similar binding pattern like the wild-type protein. For p.K1750del a reduced signal can be observed which is consistent with the effect of the alteration to the PtdInsP binding platform (see text).

200x178mm (200 x 200 DPI)